

Derivation of Pitot corrections for the Zagarola & Smits Superpipe data and their composite fit

Peter A. Monkewitz[†]

Ecole Polytechnique Fédérale de Lausanne (EPFL), CH-1015, Lausanne, Switzerland

(Received xx; revised xx; accepted xx)

Rejected by JFM Rapids, May 2018

The original turbulent pipe flow experiments in the Princeton “Superpipe” by Zagarola & Smits (1997, 1998) at unprecedented laboratory Reynolds numbers have started an ongoing vigorous debate on the logarithmic law in the mean velocity profile $U^+(y^+)$ and the intimately related question of Pitot probe corrections for mean shear, viscous effects and turbulence level. Considering that the Pitot probe diameter d^+ exceeded 7000 wall units at the highest Reynolds number, the various traditional Pitot corrections had to be extended into uncharted territory where they may no longer be additive. In this note, the inverse approach is adopted, where the net result of all the corrections is assumed to be compatible with the model for U^+ developed by Monkewitz (2017). The latter has an inner part which is, up to higher order corrections, identical to the zero pressure gradient turbulent boundary layer profile and switches around $y_{\text{break}}^+ \approx 400$ to a logarithmic overlap layer with a Kármán “parameter” κ that depends on pressure gradient and possibly on other flow parameters. The simplicity of the resulting global Pitot correction proportional to $(d^+)^{0.9}(R^+)^{-0.4}$, with only two fitting parameters, indirectly supports this model. Based on the required equality of the overlap and centerline κ 's, it is furthermore shown that y_{break}^+ must be a constant. Finally, the outer “wake” part of the profile is argued to be asymptotically linear between the wall and about half the pipe radius. This gives rise to a linear higher order tail $\propto y^+/R^+$ in the logarithmic overlap layer, which has been the subject of asymptotic analysis over the last decades.

1. The problem with the Kármán constant in pipe flow

In early pipe flow experiments, the emphasis has been on the scaling of the centerline velocity and the friction factor with Reynolds number. As measurement techniques have evolved, attention has shifted towards the “law of the wall” $U^+ = (1/\kappa)\ln(y^+) + B$, where κ is the celebrated Kármán “constant”. In the last years the value of κ in pipes has closely approached the “most popular” value of 0.384 for the zero-pressure-gradient boundary layer (Furuichi *et al.* 2015; Örlü *et al.* 2016), which seemingly supports the claim of (see e.g. Marusic *et al.* 2013; Krug *et al.* 2017, and others), that $\kappa = 0.39$ is universal for zero-pressure-gradient boundary layers, pipe and channel flows.

Here and in the following, “+” superscripts indicate non-dimensionalization with wall units $\hat{u}_\tau \equiv (\hat{\tau}_{\text{wall}}/\hat{\rho})^{1/2}$ and $\hat{\ell} \equiv \hat{v}/\hat{u}_\tau$, where hats indicate dimensional quantities. The relevant Reynolds number for pipe flow is $\text{Re}_\tau \equiv R^+ = (\hat{R}\hat{u}_\tau/\hat{v})$, with \hat{R} the pipe radius.

[†] Email address for correspondence: peter.monkewitz@epfl.ch

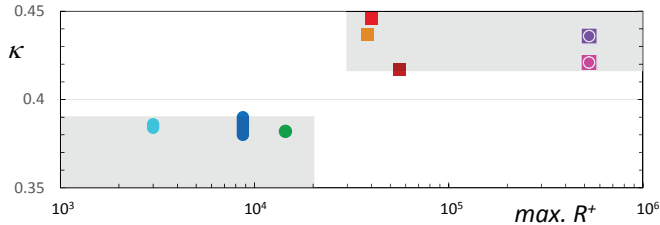


FIGURE 1. (color online) κ 's determined by different authors from near-wall $U^+(y^+)$ profiles (\bullet) and from the centerline velocity $U_{CL}^+(R^+)$ (\blacksquare) versus maximum R^+ of the respective experiment: \bullet , Monty (2005); \bullet , Zanon *et al.* (2007); \bullet , Furuichi *et al.* (2015); \blacksquare , Fiorini (2017); \blacksquare , Nagib *et al.* (2017); \blacksquare , Nikuradse (1932); \blacksquare , Zagarola & Smits (1998) and \blacksquare , McKeon *et al.* (2004). The gray boxes emphasize the separation of values obtained from low and high Reynolds number experiments.

Since the pioneering work of Coles (1956) it has been recognized that in turbulent wall-bounded flows, the logarithmic overlap layer or common part $U_{cp}^+(y^+) = \ln(y^+)/\kappa + B$ of the “inner” and “outer” asymptotic expansions of the mean velocity necessarily entails a free stream velocity $U_\infty^+(\text{Re}_\tau)$ or centerline velocity $U_{CL}^+(\text{Re}_\tau)$ of the form $\ln(\text{Re}_\tau)/\kappa + C$, with the *same* logarithmic slope ($1/\kappa$). While in the zero-pressure-gradient turbulent boundary layer, henceforth abbreviated ZPG TBL, the equality of κ 's obtained from the overlap layer and from the evolution of the free-stream velocity U_∞^+ with Reynolds number has remained non-controversial (see e.g. Monkewitz *et al.* 2007; Marusic *et al.* 2010), the κ 's extracted by different authors from pipe flow profiles have not converged to a generally agreed value, as already discussed by Nagib & Chauhan (2008) and shown in figure 1. What is striking in this figure, is the rather clear separation of reported κ values according to the Reynolds number range of the experiment: while the κ 's remain within 0.005 of the widely accepted ZPG TBL value of 0.384 for $R_{\max}^+ \lesssim 2 \times 10^4$, they jump to 0.42 and beyond in experiments with $R_{\max}^+ \gtrsim 2 \times 10^4$.

Apart from the data of Nikuradse (1932), difficult to assess, the Princeton Superpipe data were for a long time the only laboratory data beyond an R^+ of 2×10^4 and the κ 's from the log-law and from the centerline were in agreement, as they should be. However, the log-laws identified by Zagarola & Smits (1998) with $\kappa = 0.436$ and by McKeon *et al.* (2004) with $\kappa = 0.421$ only started beyond a y^+ of the order of 500, as opposed to 150 – 200 in pipe experiments at lower Reynolds numbers and in the ZPG TBL. This gave rise to extended controversies about Pitot corrections (see e.g. Perry *et al.* 2001; Bailey *et al.* 2013; Vinuesa *et al.* 2016) and to speculations about a “mixing transition” of pipe flow at $R^+ = \mathcal{O}(10^4)$ (McKeon *et al.* 2005). Only recently, Monkewitz (2017) proposed a resolution of this conundrum. He showed that in pipe and channel flows, where the effect of pressure gradient on the near-wall momentum balance is weak, mean velocity profiles are well described by the ZPG TBL profile up to $y^+ \approx 400 - 500$, implying that the pipe profile includes the beginning of the ZPG TBL log-law with $\kappa_0 = 0.384$. Beyond this wall distance, the inner pipe profile veers off to the “true” overlap log-law with a pipe-specific κ significantly higher than 0.384. Considering that beyond $Y \approx 0.05$, with $Y \equiv y^+/R^+$ the outer coordinate, the overlap log-law becomes progressively contaminated by the wake, the clean overlap log-law only becomes visible for $400 \ll 0.05R^+$, which corresponds in practice to $R^+ \gtrsim 2 \times 10^4$, as seen in figure 1.

2. The Pitot and other corrections for the Zagarola & Smits data

2.1. Roughness correction

At the higher R^+ , the Hama-like roughness correction of Monkewitz (2017)

$$\Delta U_{\text{rough}}^+ = \frac{2}{\kappa} \ln[1 + (0.14 k_s^+)^2] \quad \text{with} \quad \widehat{k}_s = 0.45 \mu\text{m} \quad , \quad (2.1)$$

has been applied, which is in line with the investigation of Allen *et al.* (2005) and significantly affects the profiles only for $R^+ \gtrsim 2 \times 10^5$.

2.2. “Reverse engineering” of the Pitot correction for the Zagarola & Smits data

The resolution of the discrepancy between κ 's from low and high Reynolds number experiments by Monkewitz (2017) is supported by the success of using his idea “backwards”, i.e. to assume that the near-wall profiles are identical in pipe and ZPG TBL, and modelled by the Musker profile modified by Chauhan *et al.* (2009):

$$U_{\text{inner}}^+(\text{ZPG}) \cong \frac{1}{\kappa_0} \ln \left(\frac{y^+ + a}{a} \right) - \frac{\gamma^2}{a(4\alpha + a)} \left\{ (4\alpha - a) \ln \left(\frac{a\sqrt{(y^+ - \alpha)^2 + \beta^2}}{\gamma(y^+ + a)} \right) + \frac{\alpha(4\alpha - 5a)}{\beta} \left[\arctan \left(\frac{y^+ - \alpha}{\beta} \right) + \arctan \left(\frac{\alpha}{\beta} \right) \right] \right\} + \frac{\exp[-\ln^2(y^+/30)]}{2.85} \quad (2.2)$$

where $\alpha = (a - 1/\kappa_0)/2$, $\beta = \sqrt{2a\alpha - \alpha^2}$ and $\gamma = \sqrt{\alpha^2 + \beta^2}$. With $\kappa_0 = 0.384$ and the parameter $a = 10.35$, the Musker profile (2.2) asymptotes to $U^+ \sim (1/0.384) \ln(y^+) + 4.21$, as in Monkewitz (2017) (Note that in appendix A of Monkewitz (2017) the above two arctan have been combined into one, which requires a branch switch at $y^+ = 20.7$, i.e. the addition of π for $y^+ \geq 20.7$).

The new global Pitot correction for the raw Superpipe data of Zagarola & Smits (1998) (available at <https://smits.princeton.edu/zagarola/> and henceforth referred to as Z&S data) is now obtained by fitting the difference $\Delta U_{\text{Pitot}}^+(\text{Z\&S}) \equiv [U_{\text{uncorr}}^+(\text{Z\&S}) - U_{\text{inner}}^+(\text{ZPG})]$ between the uncorrected Z&S data and the inner expansion in the ZPG TBL, modeled by equation (2.2). This difference $\Delta U_{\text{Pitot}}^+(\text{Z\&S})$ is found to depend logarithmically on y^+ and scale as $(d^+)^m (R^+)^{(0.5-m)} = (0.0139)^m (R^+)^{0.5}$ for the fixed ratio $d/R = 0.0139$ ($\widehat{d} = 0.9\text{mm}$) used by Zagarola & Smits (1998). As seen in figure 2a, the resulting collapse of the Z&S data is exceptionally good and nicely fitted by the simple global Pitot correction

$$\Delta U_{\text{Pitot}}^+ \equiv U_{\text{uncorr}}^+(\text{P}) - U_{\text{inner}}^+(\text{ZPG}) = 0.55 (d^+)^{0.9} (R^+)^{-0.4} \ln[1 + (0.021y^+)^{-2}] \quad (2.3)$$

The scaling of $\Delta U_{\text{Pitot}}^+(\text{Z\&S})$ with $(R^+)^{0.5}$ is further verified in figure 2b for the data below y^+ of 50, where the normalizing factor (the RHS of equ. 2.3) is sufficiently larger than the combined uncertainties of the data and of the Musker-Chauhan fit (2.2). Finally, the exponent $m \approx 0.9$ in $(d^+)^m (R^+)^{(0.5-m)}$ is found with the help of data in Appendix C of McKeon (2003), obtained with four different Pitot diameters at two R^+ of 1825 and 3328, and only corrected for static pressure errors. The normalized $\Delta U_{\text{Pitot}}^+(\text{McK})$ resulting from the choice $m = 0.9$ are seen in figure 2c to scatter considerably for $y^+ \gtrsim 50$ (even earlier for the smallest Pitot diameter of 0.3mm), but m will not be needed in the following which deals exclusively with the Z&S Superpipe data.

In conclusion, since equation (2.3) models the combined effect of different physical phenomena, no simple explanation for the proportionality of $\Delta U_{\text{Pitot}}^+$ to $(d^+)^{0.9} (R^+)^{-0.4}$ nor its logarithmic dependence on y^+ can be offered. One can only speculate about the reasons for the superior data collapse obtained by the present “black box” approach,

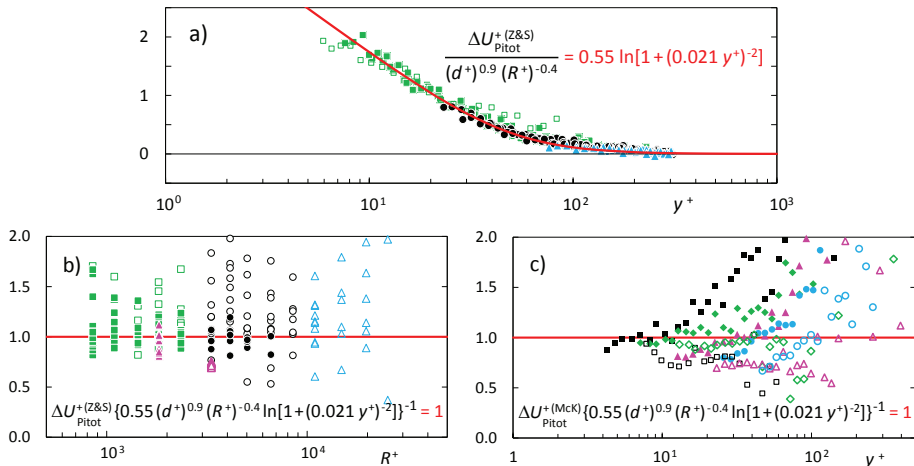


FIGURE 2. (color online) (a) Difference $\Delta U_{\text{Pitot}}^{+(Z\&S)}$ (equ. 2.3) between the uncorrected pipe velocities $U_{\text{uncorr}}^{+(Z\&S)}$ of Zagarola & Smits (1998) and the Musker-Chauhan fit $U_{\text{inner}}^{+(ZPG)}$ for the ZPG TBL inner expansion (equ. 2.2), scaled by $(d^+)^{0.9} (R^+)^{-0.4} \equiv 0.0213 (R^+)^{0.5}$. Data range $0 \leq y^+ \leq \min[300, 0.1 R^+]$ containing data up to $R^+ \approx 4 \times 10^4$. Data symbols as in fig. 3 except for the lowest $R^+ = 851$ identified by \square . —, fit by equation (2.3).

(b) Scaled difference $\Delta U_{\text{Pitot}}^{+(Z\&S)}$ versus R^+ for the Z&S data with $d/R = 0.0139$. Solid and open symbols correspond to $y^+ \leq 50$ and $50 < y^+ \leq 300$, respectively. The McKeon data of panel (c) for the same $d/R = 0.0139$ are included as purple triangles.

(c) Analogous scaled difference $\Delta U_{\text{Pitot}}^{+(McK)}$ between the data from Appendix C of McKeon (2003) and $U_{\text{inner}}^{+(ZPG)}$ versus y^+ , for $R^+ = 1825$ and Pitot O.D.'s of 0.3mm (\blacksquare), 0.5mm (\blacklozenge), 0.9mm (\blacktriangle) and 1.8mm (\bullet); Corresponding open symbols, data for $R^+ = 3328$.

as compared to the individual, physics-based corrections of Zagarola & Smits (1998), McKeon *et al.* (2003), Bailey *et al.* (2013) and Vinuesa *et al.* (2016). One possibility is that individual corrections may no longer be additive for very large d^+ , which exceed 7000 at the highest R^+ .

3. Composite expansion for the mean velocity

3.1. The inner profile

The different asymptotic regions for the data of Zagarola & Smits (1998), corrected according to equations (2.1) and (2.3), are shown in figure 3. In panel (a), only the ZPG TBL inner profile (2.2) is subtracted and the data are seen to switch around $y^+ \approx 400$ from the ZPG log-law with $\kappa_0 = 0.384$ to the “true” leading order overlap log-law with the pipe-specific $\kappa = 0.436$

$$U_{\text{cp}}^{+(P)} = \frac{1}{0.436} \ln(y^+) + 6.07 \quad (3.1)$$

which is the common part “cp” of the inner and outer expansions. Note that relative to Monkewitz (2017), the switch from the ZPG log-law to the log-law (3.1) has been lowered from 500 to 400. As an aside, the original corrected data in fig. 17 of Zagarola & Smits (1998) are seen in figure 3a to be under-corrected below $y^+ \approx 100$.

The complete leading order inner expansion for the pipe is now modelled as in

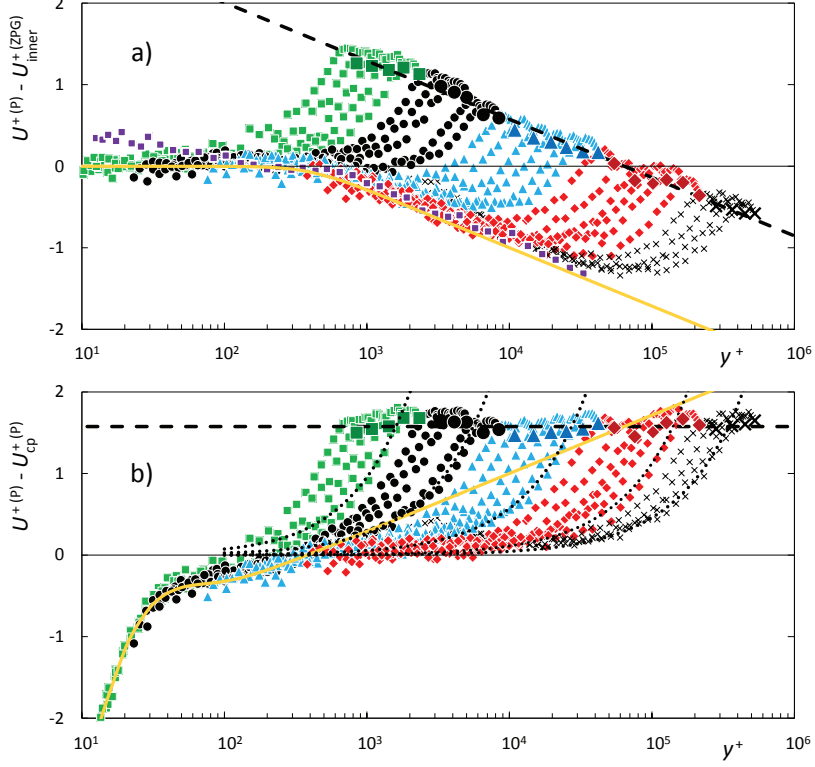


FIGURE 3. (color online) Analysis of the overlap layer of the 26 Superpipe profiles of Zagarola & Smits (1998), corrected according to equations (2.3) and (2.1), for $851 \leq R^+ \leq 528000$. \blacksquare , $R^+ < 3 \times 10^3$; \bullet , $3 \times 10^3 < R^+ \leq 10^4$; \blacktriangle , $10^4 < R^+ < 5 \times 10^4$; \blacklozenge , $5 \times 10^4 < R^+ < 2.5 \times 10^5$; \times , $2.5 \times 10^5 < R^+$ where roughness effects become significant. Corresponding large symbols mark the centerline fitted by equ. (3.3) (---).

(a) \blacksquare \bullet \blacktriangle \blacklozenge \times , $(U^+(Z\&S) - U^+(ZPG)_{inner})$ [equ. (2.2)]. \blacksquare , $U^+(Z\&S)$, taken from fig. 17 of Zagarola & Smits (1998), minus $U^+(ZPG)_{inner}$. ---, $(U^+(P) - U^+(ZPG)_{inner})$; —, $(U^+(P) - U^+(ZPG)_{inner})$ [equ. (3.2)].

(b) \blacksquare \bullet \blacktriangle \blacklozenge \times , $(U^+(Z\&S) - U^+_{cp}(P))$ [equ. (3.1)]. ---, $(U^+(P) - U^+_{cp}(P)) = 1.56$; —, $(U^+(ZPG)_{inner} - U^+_{cp}(P))$; \dots , departure $L^+(P)$ (equ. 3.6) from the log-law for the last profile in each group.

Monkewitz (2017) by

$$U^+_{inner}(P) = U^+(ZPG)_{inner} + \frac{1}{3} \left(\frac{1}{0.436} - \frac{1}{0.384} \right) \ln [1 + (0.0025 y^+)^3] \quad (3.2)$$

$$\rightarrow U^+_{cp}(P) \quad \text{for} \quad (0.0025 y^+) \gg 1 \quad ,$$

with $U^+_{cp}(P)$ given by equ. (3.1). As dictated by asymptotic matching principles, the overlap log-law (3.1) has the same $\kappa = 0.436$ as the centerline log-law

$$U^+_{CL}(P) = \frac{1}{0.436} \ln(R^+) + 7.63 \quad . \quad (3.3)$$

This is again evident in figure 3b, where only the common part $U^+_{cp}(P)$ (equ. 3.1) has been subtracted from the data to show the excellent collapse of all the data below $y^+ \approx 400$

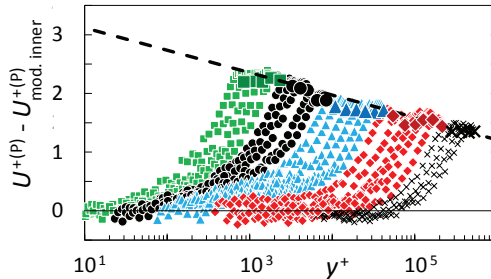


FIGURE 4. (color online) Same data as in fig. 3 minus $U_{inner}^{+(Z\&S)}$ with a breakpoint between the remnant of the ZPG log-law and the pipe overlap log-law modified from $(0.0025 y_{break}^+) = 1$ to $0.7 y_{break}^+ / (R^+)^{1/2} = 1$ in equation (3.2). - - -, resulting centerline $\kappa_{CL} = 0.47$.

onto the Musker-Chauhan profile (2.2), as intended with the correction scheme of section 2.2.

Finally, in view of the different proposals for the start of the pipe overlap log-law, for instance $y_{break}^+ / (R^+)^{1/2} = 3$ proposed by Marusic *et al.* (2013) and others, the present scaling $(0.0025 y_{break}^+) = 1$ for the start of the overlap log-law in equation (3.2) and figure 3a requires a closer examination. Replacing $[0.0025 y^+]$ in the logarithm of equation (3.2) by $[0.7 y^+ (R^+)^{-0.5}]$, for instance, modifies figure 3b to figure 4, where $\kappa_{CL} = 0.47$ is no longer equal to the overlap κ of 0.436, as required by the leading order matching between the overlap and outer profiles. The reason for this is easily identified by evaluating the limit of the modified equation (3.2) for $(0.7 y^+ / \sqrt{R^+}) \gg 1$, resulting in a modification of the common part (equ. 3.1) to $(1/0.436) \ln(y^+) + 4.31 + 0.16 \ln(R^+)$. Subtracting this modified common part from the data yields a wake function which decreases as $0.16 \ln(R^+)$ on the centerline, corresponding to a centerline kappa of $[(1/0.436) - 0.16] \ln(R^+) = 0.47 \ln(R^+)$, as seen in figure 4. This argument against a Reynolds number dependent y_{break}^+ , i.e. the lower end of the overlap log-law, is independent of the actual value of the overlap kappa and the power $p \neq 0$ of R^+ in $[y_{break}^+ (R^+)^{-p}] = \text{constant}$. In practice, the problem “disappears” in the data uncertainty for sufficiently small p , but must remain of concern when speculating about the infinite Reynolds number limit.

3.2. The linear part of the outer “wake” profile

Driven by the desire to obtain more reliable values for the Kármán parameter from data at moderate Reynolds numbers, Yajnik (1970), Afzal (1976, 1996), Jiménez & Moser (2007) and Luchini (2017), among others, have proposed various higher order corrections to the log-law, notably linear corrections $\propto y^+ / R^+$. While most of these proposed corrections were justified by asymptotic matching arguments, it is argued here that the linear correction in the overlap layer is just the tail of the linear part of the outer wake profile, and therefore dependent on the outer boundary conditions. This is demonstrated with the pipe DNS of El Khoury *et al.* (2013). It is straightforward to determine the effective turbulent viscosity from the momentum equation and the computed mean velocity derivative. Beyond the inner region it is, in outer variables, equal to $N_T \equiv \nu_T^+ / R^+ = (1 - Y)(dU^+ / dY)^{-1}$ (see e.g. Wilcox 1993, section 3.5). As shown in figure 5a, N_T is well fitted by

$$N_T = 0.048 + 0.122(1 - Y)^2 - 0.17(1 - Y)^4 \cong 0.436Y - 0.898Y^2 + \mathcal{O}(Y^3) \text{ for } Y \ll 1. \quad (3.4)$$

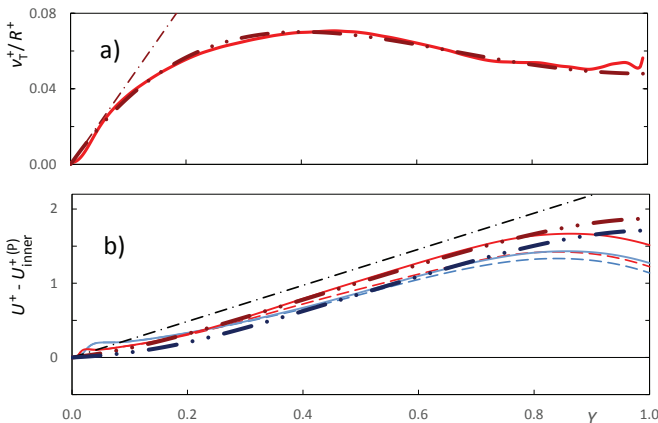


FIGURE 5. (color online) (a) —, turbulent viscosity $N_T \equiv \mu_T^+/R^+$, calculated from the DNS of El Khoury *et al.* (2013) for $R^+ = 999$; - - -, $0.436Y$; - · · -, fit (3.4). (b) DNS mean velocity profiles of El Khoury *et al.* (2013) for $R^+ = 550$ (—) and $R^+ = 999$ (—) minus $U_{\text{inner}}^{+(P)}$ (equ. 3.2); - - -, corresponding profiles minus $U_{\text{inner}}^{+(ZPG)}$ (equ. 2.2); - · · -, $L^{+(P)}$ fitted by equation (3.6) for $R^+ = 550$ and 999 ; - · · -, limit $2.43Y$ at $R^+ = \infty$ (without the slope decrease towards the CL).

For small Y , the fit (3.4) corresponds to

$$U^+ = \ln Y/0.436 + C + 2.43Y + \mathcal{O}(Y^2) \quad \text{for } Y \ll 1. \quad (3.5)$$

From figure 5b it is obvious that the linear term in equation (3.5) needs to be offset by an estimated $(80/R^+)$ to obtain good fits at the lower R^+ . This is achieved by the construction

$$L^{+(P)} = \frac{1}{c_s} \ln \left[1 - e^{-2.43 c_s Y_0} + e^{2.43 c_s (Y - Y_0)} \right] - 2.43 F_3(Y) \quad \text{with} \quad (3.6)$$

$$c_s = 5, Y_0 = 80/R^+ \quad \text{and} \quad F_n(Y) \equiv \frac{1}{n \ln^{n-1} \left(\frac{\pi}{2} \right)} \left\{ \ln \left[\frac{\pi}{2} Y \right] - \ln \left[\sin \left(\frac{\pi}{2} Y \right) \right] \right\}^n, \quad (3.7)$$

where $c_s < \infty$ smoothes the corner at $Y = Y_0$ and the constants in the argument of the logarithm in equation (3.6) ensure that $L^{+(P)}(0) = 0$. For large R^+ , the first logarithmic term of $L^{+(P)}$ quickly approaches the straight line $2.43Y$, shown in figure 5b. The zero centerline slope $(dL^{+(P)}/dY)(1) = 0$ is obtained with the function $F_n(Y)$ which has a slope of unity on the centerline and is proportional to Y^{2n} for $Y \ll 1$. The choice of F_3 in equation (3.6) ensures that, after the offset by $(80/R^+)$, $L^{+(P)}$ remains linear up to $Y \approx 0.5$.

It is noted in passing that the two wake profiles in figure 5b, obtained from the DNS of El Khoury *et al.* (2013), show some suspicious ‘‘humps’’ near the origin. They are clearly the result of an imperfect ‘‘overshoot’’ term in the Musker-Chauhan fit, the last term of equation (2.2), which should go to zero faster below $y^+ = 30$ and be higher at these low R^+ . However, since the appropriate higher order corrections in the inner region, presumably of $\mathcal{O}(1/R^+)$ like the quadratic term $-(y^+)^2/(2R^+)$ in the Taylor expansion of U^+ about the origin, have no direct bearing on the present analysis, no effort has been made here to improve equation (2.2).

The present construction of the linear term in the outer expansion shows that its coefficient depends on the entire outer shape of the turbulent viscosity N_T and not on some matching condition in the overlap layer. For pipe and channel, N_T must be

symmetric about the centerline. Assuming that it can be represented as a polynomial in powers of $(1 - Y)^2$, as in equation (3.4), a linear term in the outer velocity profile is unavoidable, except in the unlikely case that the coefficients of all the Y^2 -terms of N_T sum up to $-\kappa$. The situation is different for the ZPG TBL where the departure from the log-law is $\propto Y^4$, according to the data analysis of Monkewitz (2017), implying a small- Y expansion of N_T of the form $\kappa_0 Y + \mathcal{O}(Y^5)$.

The discussion on how the slope of 2.43 for the linear part of the pipe wake might be connected to the pressure gradient parameter $\beta = -\widehat{R} \widehat{p}_x / \widehat{\tau}_{\text{wall}}$ is postponed to the concluding section 4.

3.3. The complete outer pipe profile

The obvious question is now whether the term $L^{+(P)}$ of equation (3.6), deduced from the DNS of El Khoury *et al.* (2013), also “works” for the Z&S data. Figure 6a shows that it does, and that the Z&S data all fall between the $L^{+(P)}$ for the lowest R^+ of 850 and $R^+ = \infty$. Since the data scatter in figure 6a is of the same magnitude as the difference between these two $L^{+(P)}$, only an average $L^{+(P)}$ corresponding to $R^+ = 2000$ is subtracted from the data to obtain figure 6b which shows that the pipe wake is well described by $L^{+(P)}$, i.e. is linear in the interval $2Y_0 \lesssim Y \lesssim 0.5$.

The last step towards the composite expansion is to compensate the centerline slope of $-(1/\kappa)$ caused by the log-law in $U_{\text{inner}}^{+(P)}$. This is easily achieved by adding $(1/0.436)F_3(Y)$ to the data of figure 6b, resulting in the rather satisfactory fit of $U_{\text{comp}}^{+(P)}$ shown in figure 6c, and given by

$$U_{\text{comp}}^{+(P)} = U_{\text{inner}}^{+(P)} + U_{\text{outer}}^{+(P)} - U_{\text{cp}}^{+(P)} \quad \text{with} \quad (3.8)$$

$$U_{\text{wake}}^{+(P)} \equiv U_{\text{outer}}^{+(P)} - U_{\text{cp}}^{+(P)} = L^{+(P)}(Y; R^+ = 2000) + (1/0.436) F_3(Y), \quad (3.9)$$

with F_3 defined by equation (3.7). It is worth reiterating here that the leading behavior of the present wake fit (3.9) is **linear** in Y , with a higher order offset. This is qualitatively different from previous fits, including the one in Monkewitz (2017), which were all variations of Coles’ \sin^2 wake function, i.e. $\propto Y^2$ for small Y . Only at low R^+ there is some resemblance between the new and the traditional pipe wake functions due to the offset in equation (3.6).

4. Conclusions

In conclusion, the extreme simplicity of the present Pitot correction of the original Superpipe data of Zagarola & Smits (1998) strongly supports the notion of Monkewitz (2017) that the near-wall velocity profile in the pipe is, within experimental uncertainty and up to small $\mathcal{O}(1/R^+)$ corrections, equal to the ZPG TBL profile out to $y_{\text{break}}^+ \approx 400 - 500$, where the pipe profile switches to the overlap log-law (3.1) with a pipe-specific Kármán parameter κ of 0.436. Comparing with the Superpipe data of McKeon *et al.* (2004) used in Monkewitz (2017), the difference between overlap κ 's - 0.436 versus 0.421 - is on the high side of uncertainty estimates (see e.g. Bailey *et al.* 2014). One reason may be that the data set of Zagarola & Smits (1998) contains more low Reynolds number profiles than the one of McKeon *et al.* (2004). Eliminating the Z&S profiles below $R^+ = 10^4$ does reduce their centerline κ_{CL} from 0.436 to 0.430, but in view of the increasing uncertainty of the Pitot corrections with Reynolds number and the centerline κ_{CL} of 0.446 recently found in the CICLoPE pipe by Nagib *et al.* (2017), the original overlap κ of 0.436 appears to be a reasonable value for the pipe and has been maintained for the present analysis.

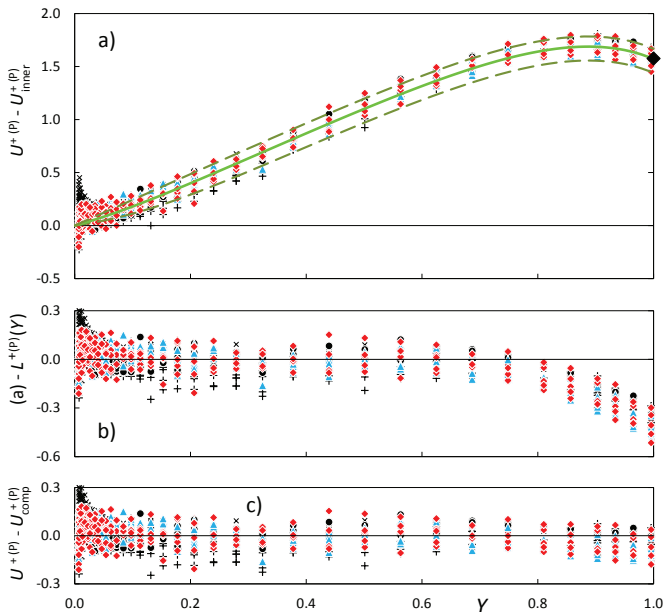


FIGURE 6. (color online) (a) The wake function $U_{\text{wake}}^{+(\text{P})}(Y)$ of equation (3.9) with the same data and color coding as in figure 3; $- - -$, $—$, $- \cdot - \cdot -$, asymptotically linear part $L^{+(\text{P})}$ in equation (3.6) for $R^+ = 850, 2000$ and ∞ ; \blacklozenge , $U_{\text{CL}}^{+(\text{P})}$ [equ. 3.3] minus $U_{\text{inner}}^{+(\text{P})}(y^+ = R^+)$. (b) $U_{\text{wake}}^{+(\text{P})}(Y) - L^{+(\text{P})}(Y; R^+ = 2000)$. (c) Complete fit $U^{+(\text{Z\&S})} - U_{\text{comp}}^{+(\text{P})}$ [equs. (3.8), (3.9)].

The important finding here is that the sequence of asymptotic regions is the **same** for the two Superpipe data sets and the structure of the fitting functions for the different asymptotic regions is identical to the one in Monkewitz (2017), despite the different κ 's. The substantial difference to previous fits is the new wake function which is asymptotically linear over about half the pipe radius and represents a radical departure from the traditional \sin^2 type function, originally introduced by Coles (1956). This asymptotically linear outer departure from the log-law suggests that the linear higher order corrections to the log-law (see e.g. Luchini 2017, and references therein) are slaved to the outer expansion and not an intrinsic consequence of asymptotic matching.

It is now natural to ask if and how the slope of $L^{+(\text{P})}$ is related to the pressure-gradient parameter $\beta = -\widehat{R}\widehat{p}_x/\widehat{\tau}_{\text{wall}}$. Since the wake of ZPG TBL's shows no linear part, it is tempting to make the slope of $L^{+(\text{P})}$ proportional to β , at least for $\beta \leq \mathcal{O}(1)$. However, the geometry and in particular transverse wall curvature are known to also modify the asymptotic structure and are therefore expected to contribute to the slope of $L^{+(\text{P})}$ in a non-trivial way. In particular flat plate TBL's in weak pressure gradients are expected to have a linear wake part different from pipe and channel, because of the different free stream boundary conditions for the turbulent viscosity N_T .

To close the discussion, the channel DNS of Lee & Moser (2015) for $H^+ = 5200$ is reanalyzed with the methodology of the present paper. Maintaining the overlap κ at 0.413 as in Monkewitz (2017), but shifting the break between the ZPG and channel log-laws to $y^+ = 500$ yields the wake profile of figure 7. As for the pipe, it is first fitted by

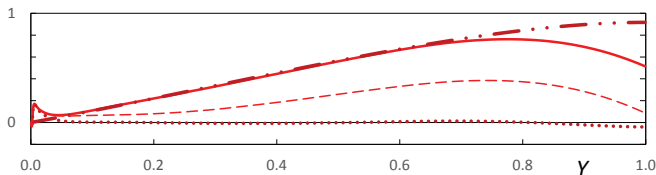


FIGURE 7. (color online) —, DNS mean velocity profile $U^{+(\text{L\&M})}$ of Lee & Moser (2015) for $H^+ = 5200$ minus $U_{\text{inner}}^{+(\text{Ch})}$; - - -, DNS profile minus $U_{\text{inner}}^{+(\text{ZPG})}$ (equ. 2.2); - · - · -, $L^{+(\text{Ch})}$ fitted by equation (4.1); · · · ·, $U^{+(\text{L\&M})} - U_{\text{comp}}^{+(\text{Ch})}$. For an explanation of the nonphysical “hump” near the origin, see the comment in section 3.2 regarding the same phenomenon in figure 5b.

$L^{+(\text{Ch})}$, given by

$$L^{+(\text{Ch})} = \frac{1}{c_s} \ln \left[1 - e^{-1.23 c_s Y_0} + e^{1.23 c_s (Y - Y_0)} \right] - 1.23 F_2(Y) \quad \text{with } c_s = 5, Y_0 = 150/H^+ \quad (4.1)$$

with F_2 defined by equation (3.7). Adding just $(1/0.413)F_3(Y)$ to fix the centerline slope leads to a near perfect composite fit. It is intriguing to find that the slopes of the linear wake component in pipe and channel, fitted here as 2.43 and 1.23, are related by a factor of 2. It is left to the reader to speculate whether the two slopes should be fitted by 1.22β or by a more complicated function of β , transverse wall curvature, $\kappa(\beta)$ or other parameters.

The author is most grateful to Hassan Nagib for his helpful comments on various points addressed in this paper.

REFERENCES

- AFZAL, NOOR 1976 Millikans argument at moderately large reynolds number. *The Physics of Fluids* **19** (4), 600–602.
- AFZAL, NOOR 1996 Wake layer in a turbulent boundary layer with pressure gradient : a new approach. In *IUTAM Smposium on Asymptotic Methods for Turbulent Shear Flows at High Reynolds Numbers* (ed. K. Gersten), pp. 95–118. Kluwer Academic Publishers.
- ALLEN, J. J., SHOCKLING, M. A. & SMITS, A. J. 2005 Evaluation of a universal transitional resistance diagram for pipes with honed surfaces. *Phys. Fluids* **17**, 121702.
- BAILEY, S. C. C., HULTMARK, M., MONTY, J. P., ALFREDSSON, P. H., CHONG, M. S., DUNCAN, R. D., FRANSSON, J. H. M., HUTCHINS, N., MARUSIC, I., MCKEON, B. J., NAGIB, H. M., ÖRLÜ, R., SEGALINI, A., SMITS, A. J. & VINUESA, R. 2013 Obtaining accurate mean velocity measurements in high Reynolds number turbulent boundary layers using Pitot tubes. *J. Fluid Mech.* **715**, 642–670.
- BAILEY, S. C. C., VALLIKIVI, M., HULTMARK, M. & SMITS, A. J. 2014 Estimating the value of von Kármán’s constant in turbulent pipe flow. *J. Fluid Mech.* **749**, 79–98.
- CHAUHAN, K. A., MONKEWITZ, P. A. & NAGIB, H. M. 2009 Criteria for assessing experiments in zero pressure gradient boundary layers. *Fluid Dynamics Research* **41** (2), 021404.
- COLES, D. E. 1956 The law of the wake in the turbulent boundary layer. *J. Fluid Mech.* **1**, 191–226.
- EL KHOURY, GEORGE K., SCHLATTER, PHILIPP, NOORANI, AZAD, FISCHER, PAUL F., BRETHOUWER, GEERT & JOHANSSON, ARNE V. 2013 Direct numerical simulation of turbulent pipe flow at moderately high reynolds numbers. *Flow, Turbulence and Combustion* **91** (3), 475–495.
- FIORINI, TOMMASO 2017 Turbulent pipe flow - high resolution measurements in CICLoPE. PhD thesis, University of Bologna.
- FURUICHI, N., TERAQ, Y., WADA, Y. & TSUJI, Y. 2015 Friction factor and mean velocity profile for pipe flow at high Reynolds numbers. *Phys. Fluids* **27** (9), 095108.

- JIMÉNEZ, JAVIER & MOSER, ROBERT D 2007 What are we learning from simulating wall turbulence? *Phil. Trans. R. Soc. A* **365** (1852), 715–732.
- KRUG, DOMINIK, PHILIP, JIMMY & MARUSIC, IVAN 2017 Revisiting the law of the wake in wall turbulence. *J. Fluid Mech.* **811**, 421–435.
- LEE, M. & MOSER, R. D. 2015 Direct numerical simulation of turbulent channel flow up to $Re_\tau = 5200$. *J. Fluid Mech.* **774**, 395–415.
- LUCHINI, PAOLO 2017 Universality of the turbulent velocity profile. *Phys. Rev. Lett.* **118**, 224501.
- MARUSIC, I., MCKEON, B. J., MONKEWITZ, P. A., NAGIB, H. M., SMITS, A. J. & SREENIVASAN, K. R. 2010 Wall-bounded turbulent flows at high Reynolds numbers: Recent advances and key issues. *Phys. Fluids* **22**, 065103: 1–24.
- MARUSIC, I., MONTY, J. P., HULTMARK, M. & SMITS, A. J. 2013 On the logarithmic region in wall turbulence. *J. Fluid Mech. Rapids* **716**, R3–1–R3–11.
- MCKEON, BEVERLEY J. 2003 High Reynolds number turbulent pipe flow. PhD thesis, Princeton University.
- MCKEON, B. J., LI, J., JIANG, W., MORRISON, J. F. & SMITS, A. J. 2003 Pitot probe corrections in fully-developed turbulent pipe flow. *Meas. Sci. Tech.* **14** (8), 1449–1458.
- MCKEON, B. J., LI, J., JIANG, W., MORRISON, J. F. & SMITS, A. J. 2004 Further observations on the mean velocity distribution in fully developed pipe flow. *J. Fluid Mech.* **501**, 135–147.
- MCKEON, B. J., ZAGAROLA, M. V. & SMITS, A. J. 2005 A new friction factor relationship for fully developed pipe flow. *J. Fluid Mech.* **538**, 429–443.
- MONKEWITZ, PETER A. 2017 Revisiting the quest for a universal log-law and the role of pressure gradient in “canonical” wall-bounded turbulent flows. *Phys. Rev. Fluids* **2**, 094602.
- MONKEWITZ, P. A., CHAUHAN, K. A. & NAGIB, H. M. 2007 Self-consistent high-Reynolds-number asymptotics for zero-pressure-gradient turbulent boundary layers. *Phys. Fluids* **19**, 115101.
- MONTY, J. P. 2005 Developments in smooth wall turbulent duct flows. PhD thesis, University of Melbourne.
- NAGIB, H. M. & CHAUHAN, K. A. 2008 Variations of von Kármán coefficient in canonical flows. *Phys. Fluids* **20**, 101518.
- NAGIB, H. M., MONKEWITZ, P. A., MOSCOTELLI, L., FIORINI, T., BELLANI, G., ZHENG, X. & TALAMELLI, A. 2017 Centerline Kármán ‘constant’ revisited and contrasted to log-layer Kármán constant at CICLoPE. In *Proc. TSFP10, Chicago, USA* (ed. H. M. Nagib & A. J. Smits).
- NIKURADSE, J. 1932 Gesetzmässigkeiten der turbulenten Strömung in glatten Röhren. [English translation: NASA TT F-10, 359]. *VDI Forschungsheft no. 356* .
- ÖRLÜ, R., FIORINI, T., SEGALINI, A., BELLANI, G., TALAMELLI, A. & ALFREDSSON, P. H. 2016 Reynolds stress scaling in pipe flow turbulence - first results from CICLoPE. *Phil. Trans. R. Soc. A* **375**, 20160187.
- PERRY, A. E., HAFEZ, S. & CHONG, M. S. 2001 A possible reinterpretation of the princeton superpipe data. *Journal of Fluid Mechanics* **439**, 395401.
- VINUESA, R., DUNCAN, R. D. & NAGIB, H. M. 2016 Alternative interpretation of the superpipe data and motivation for ciclope: The effect of decreasing viscous length scale. *Eur. J. of Mech. - B/Fluids* **58**, 109–116.
- WILCOX, DAVID C. 1993 *Turbulence Modeling for CFD*. DCW Industries.
- YAJNIK, KIRIT S. 1970 Asymptotic theory of turbulent shear flows. *Journal of Fluid Mechanics* **42** (2), 411427.
- ZAGAROLA, M. V. & SMITS, A. J. 1997 Scaling of the mean velocity profile for turbulent pipe flow. *Phys. Rev. Letters* **78**, 239–242.
- ZAGAROLA, M. V. & SMITS, A. J. 1998 Mean-flow scaling of turbulent pipe flow. *J. Fluid Mech.* **373**, 33–79.
- ZANOUN, E. S., DURST, F., BAYOUMY, O. & AL-SALAYMEH, A. 2007 Wall skin friction and mean velocity profiles of fully developed turbulent pipe flows. *Exp. Thermal and Fluid Sci.* **32** (1), 249–261.